

AUGMENTED LAGRANGIAN TECHNIQUE APPLIED TO A SPATIALLY PERIODIC, HARMONIC NAVIER–STOKES PROBLEM

LIONEL BORNE

Ecole Nationale des Travaux Publics de l'Etat, Rue Maurice Audin, 69120 Vaulx en Velin, France

and

Institut de Mecanique de Grenoble, UA6 C.N.R.S., BP. No. 68, 38402 Saint Martin D'Herès Cedex, France

SUMMARY

An application and an extension (to complex variables) of the classical augmented Lagrangian method is performed. Finite element computations are realized in the two-dimensional case of an harmonic Navier–Stokes problem with periodic boundary conditions. A formulation (extended from the traditional Stokes problem) involving a simple Lagrangian, solved by the Uzawa algorithm, was previously used.¹ This treatment proved unsatisfactory for large frequencies. The efficient and well-known augmented Lagrangian technique solved by the Uzawa algorithm is used to overcome these shortcomings. Other, better techniques could be used. Nevertheless the simple method used here is efficient. Moreover the numerical implementation needs little memory storage, which is an important factor in this particular case. The well-known conditioning technique employed is shown to be well-adapted in this case, a fact which emerges from the study of the non-symmetric problem involved. Finally, many tests, computations and experimental data are presented.

KEY WORDS Navier–Stokes Problem Augmented Lagrangian Method Uzawa Algorithm Conforming Finite Element Methods

INTRODUCTION

This paper shows the efficiency, for one very particular case, of augmented Lagrangian techniques. The convergence of the Uzawa algorithm applied to this formulation is here studied numerically (non-symmetrical problem). These traditional techniques are extended to unknown functions with complex values, and the resulting structure is well-adapted to the conditioning technique employed.

First, all working assumptions and the problem to be solved will be briefly reviewed, along with the results obtained with the usual Lagrangian formulation. Up to this point, the problem to be solved remains unchanged and we conclude that the Lagrangian formulation solved by the Uzawa algorithm does not allow computations for large frequencies.¹

Subsequently, we recall the augmented Lagrangian formulation applied to a usual homogeneous Stokes problem.² This technique is then extended and applied to our problem. After a reminder of the two discrete problems which were used in Reference 1 and which are used here, the suitability of the method is stressed.

A theoretical study of the convergence of the Uzawa algorithm is possible for the classical homogeneous Stokes problem.² Results will be recalled in the second part of this paper. It is to be

noted that theoretical results are not available for non-symmetric problems. Therefore, tests on a simple case are performed and numerical solutions are compared to theoretical ones.

Finally computations on a severe geometrical example are presented and compared with previous computational results, asymptotic behaviour results, and experimental data.

WORKING ASSUMPTIONS, THE PROBLEM TO BE SOLVED AND FIRST RESULTS

It should be pointed out that all of the following section is a summary of a previous paper.¹

Working assumptions

The physical problem is the dynamic (harmonic only) filtration of a Newtonian fluid through a porous medium.

Geometrical context

- (a) Two dimensional problem: only media where filtration can be studied in two dimensions are taken into account.
- (b) Periodic problem: the medium comprises a set of identical elementary periods Ω . The study is then limited to one period with periodic boundary conditions on parameters and with unknown functions. This property is called Ω -periodicity. Two periods are sketched in Figure 1.

Assumptions regarding the fluid. The fluid is assumed to be viscous, Newtonian and incompressible.

Assumption regarding the skeleton. It is rigid, and so will not lose its shape.

Other assumptions. The Reynolds number of the flow is very low: convective terms in Navier-Stokes equations are negligible.

Notations and problem to be solved

Under these assumptions and the notations below, the problem to be solved is written: find the

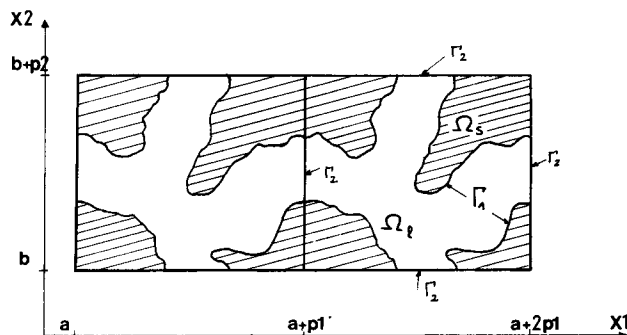


Figure 1. Two periods Ω of a porous medium: Ω_1 = fluid domain; Ω_s = solid domain; Γ_1 = fluid-solid interface

fields v and p in Ω_1 so that

$$\mu \frac{\partial^2 v_j}{\partial x_k \partial x_k} + \frac{\partial p}{\partial x_j} + F_j = i\omega\rho v_j, \tag{1a}$$

$$\frac{\partial v_j}{\partial x_j} = 0 \tag{1b}$$

and

$$v_j = 0 \text{ on } \Gamma_1, v_j \text{ and } p \text{ } \Omega\text{-periodic on } \Gamma_2 \text{ (} j = 1, 2), \tag{1c}$$

where ρ is the fluid mass per unit of volume, μ is the dynamic viscosity, v_j is the velocity component (Ω -periodic unknown functions with complex values), p is the pressure (Ω -periodic unknown functions with complex values), x_j is the spatial variable $j = 1, 2$, F_j is a constant body force (real constant), ω is the constant pulsation, i is the pure imaginary number.

The formulation (1), with complex unknown functions, is quite usual in the case of an harmonic study. The unknown functions are the complex amplitude of the true unknowns functions. (1) is analogous to the Navier–Stokes equations.

Previous computations and conclusions

Problem (1) is a particular, linear Navier–Stokes problem with complex unknown functions and Ω -periodic boundary conditions.

The numerical treatment of the periodic boundary condition is not recalled here¹ and will remain unchanged. Problem (1) was treated¹ by extending the traditional Lagrangian formulation, solved with the Uzawa algorithm.²⁻⁴ Two kinds of conforming finite elements were employed.⁵

Whereas in the static case ($\omega = 0$, periodic Stokes problem), or for small values of ω , good results were obtained; for large values of the pulsation ω , it becomes impossible to reach results, since the convergence of the Uzawa algorithm is very slow. Our purpose in what follows is to overcome this limit at lower cost and attempt to explain this behaviour.

THE AUGMENTED LAGRANGIAN METHOD

This method, presented in Reference 2 for the traditional homogeneous Stokes problem, is now a well-known efficient preconditioning technique. We first recall the main results for the homogeneous Stokes problem.² A theoretical (spectral) study of the convergence of the Uzawa algorithm is possible. The matrix of the linear system is symmetric positive definite.

As in Reference 1, by extension to our periodic, harmonic problem, we will also underline the suitability of the augmented Lagrangian to our problem, and to similar kinds of problems.

The homogeneous Stokes problem

If we replace (1c) by homogeneous boundary conditions and we take ω to be zero in (1a) we obtain the homogeneous Stokes problem:

$$\mu \frac{\partial^2 v_j}{\partial x_k \partial x_k} + \frac{\partial p}{\partial x_j} + F_j = 0 \tag{2a}$$

$$\left. \begin{array}{l} \\ \frac{\partial v_j}{\partial x_j} = 0 \end{array} \right\} \forall M \Omega_1, \tag{2b}$$

$$v_j = 0, \forall M \in \partial\Omega_1 \text{ (boundary of } \Omega \text{) } (j = 1, 2). \quad (2c)$$

At this stage, note that all components in these equations have real values. Some classical definitions

$$L^2(\Omega_1) = \left\{ f: \Omega_1 \rightarrow \mathbb{R} \mid \int_{\Omega_1} f^2 \, d\Omega \text{ exists} \right\}$$

is a Hilbert space with the scalar product

$$\forall f, g \in L^2(\Omega_1); \quad (f, g) = \int_{\Omega_1} f \cdot g \, d\Omega.$$

$$H^1(\Omega_1) = \left\{ f \in L^2(\Omega_1) \mid \frac{\partial f}{\partial x_j} \in L^2(\Omega_1); j = 1, 2 \right\}$$

is a traditional Sobolev space with the norm induced by

$$\forall f, g \in L^2(\Omega_1); \quad (f, g) = \int_{\Omega_1} \left(f \cdot g + \frac{\partial f}{\partial x_j} \frac{\partial g}{\partial x_j} \right) d\Omega.$$

$$H_0^1 = \{ v \in H^1(\Omega_1) \mid v|_{\partial\Omega} = 0 \}$$

is a Hilbert space with the scalar product

$$\forall \alpha, v \in H_0^1; \quad ((\alpha, v)) = \int_{\Omega_1} \frac{\partial \alpha}{\partial x_j} \frac{\partial v}{\partial x_j} \, d\Omega.$$

And finally the subspace V is defined by

$$V = \{ \mathbf{v} \in (H_0^1(\Omega_1))^2 \mid \text{div } \mathbf{v} = 0 \}$$

with the scalar products

$$\forall \alpha, \mathbf{v} \in V; \quad ((\alpha, \mathbf{v})) = \int_{\Omega_1} \frac{\partial \alpha_i}{\partial x_j} \frac{\partial v_i}{\partial x_j} \, d\Omega,$$

$$(\alpha, \mathbf{v}) = \int_{\Omega_1} \alpha_j v_j \, d\Omega.$$

So we now have the usual weak formulation equivalent to (2): find $\mathbf{v} \in V$ so that

$$\forall \alpha \in V; \quad \mu((\alpha, \mathbf{v})) = (\alpha, \mathbf{F}). \quad (3)$$

Let $J(\mathbf{v})(\mathbf{v} \in V)$ now be the quadratic form

$$J(\mathbf{v}) = \frac{\mu}{2}((\mathbf{v}, \mathbf{v})) - (\mathbf{F}, \mathbf{v}),$$

equation (3) is then equivalent to the minimization problem: find $\mathbf{v} \in V$ so that

$$\forall \mathbf{u} \in V; \quad J(\mathbf{v}) \leq J(\mathbf{u}). \quad (4)$$

This minimization problem under the constraint $\mathbf{v} \in V$, is then usually transformed into an equivalent saddle-point problem by the use of the Lagrangian $\mathcal{L}^{2,3}$ defined by

$$\forall \mathbf{v} \in (H_0^1(\Omega_1))^2; \quad \forall p \in L^2(\Omega_1); \quad \mathcal{L}(\mathbf{v}, p) = \frac{\mu}{2}((\mathbf{v}, \mathbf{v})) - (\mathbf{F}, \mathbf{v}) + (p, \text{div } \mathbf{v}).$$

The equivalent saddle-point problem is written: find $\mathbf{v} \in (H_0^1(\Omega_1))^2$, and $p \in L^2(\Omega_1)$ so that

$$\forall \mathbf{u} \in (H_0^1(\Omega_1))^2; \quad \forall q \in L^2(\Omega_1); \quad \mathcal{L}(\mathbf{v}, q) \leq \mathcal{L}(\mathbf{v}, p) \leq \mathcal{L}(\mathbf{u}, p). \tag{5}$$

The numerical treatment used in Reference 1 is an extension of this formulation (5).

Discrete approximations of the spaces $(H_0^1(\Omega_1))^2$ and $L^2(\Omega_1)$ (or the analogous complex spaces for our extension) are possible, and the corresponding discrete problem is then solved by using the Uzawa algorithm.

Nevertheless (5) can be replaced by another equivalent saddle-point problem using the augmented Lagrangian \mathcal{L}_r .²

The study made in Reference 2 shows that this refinement applied to the usual homogeneous Stokes problem increases the convergence of the Uzawa algorithm. The augmented Lagrangian \mathcal{L}_r is defined as

$$\begin{aligned} &\forall \mathbf{v} \in (H_0^1(\Omega_1))^2; \quad \forall p \in L^2(\Omega_1); \\ &\mathcal{L}_r(\mathbf{v}, p) = \mathcal{L}(\mathbf{v}, p) + r(\operatorname{div} \mathbf{v}, \operatorname{div} \mathbf{v}), \\ &\mathcal{L}_r(\mathbf{v}, p) = \frac{\mu}{2}((\mathbf{v}, \mathbf{v})) - (\mathbf{F}, \mathbf{v}) + (p, \operatorname{div} \mathbf{v}) + r(\operatorname{div} \mathbf{v}, \operatorname{div} \mathbf{v}), \end{aligned}$$

where r is a parameter to be chosen.

The equivalent saddle-point problem is written: find $\mathbf{v} \in (H_0^1(\Omega_1))^2$ and $p \in L^2(\Omega_1)$ so that

$$\forall \mathbf{u} \in (H_0^1(\Omega_1))^2; \quad \forall q \in L^2(\Omega_1); \quad \mathcal{L}_r(\mathbf{v}, q) \leq \mathcal{L}_r(\mathbf{v}, p) \leq \mathcal{L}_r(\mathbf{u}, p). \tag{6}$$

It is to be noted that the Uzawa algorithm can be directly applied to this continuous problem (6), as it was by Temam³ in the case $r = 0$. In practice, this means that the rate of convergence of the Uzawa algorithm must bear no relation to the refinement of the mesh employed. Nevertheless, we need to build a discrete approximated problem, in order to obtain numerical results.

Several approximations of the spaces $(H_0^1(\Omega_1))^2$ and $L^2(\Omega_1)$ are available in the literature. We may now recall just two convergent approximations that were previously used¹ and that will be used again, which are both conforming finite element methods.⁵ It is known that to obtain a convergent approximation, they must satisfy the Babuska–Brezzi condition.^{6,7} This means that the finite space W approximating $(H_0^1(\Omega_1))^2$ and Q approximating $L^2(\Omega_1)$ must be chosen with care. Or in other words, the incompressibility condition will be partially satisfied. With the spaces W and Q we need to build a discrete divergence operator. In the following it will be denoted by div_h . Table I briefly recalls the two kinds of Crouzeix–Raviart elements⁵ used. Note that the h index indicates discrete quantities.

Problem (6) is then approximated to: find $\mathbf{v}_h \in W$ and $p_h \in Q$ so that

$$\forall \mathbf{u} \in W \quad \text{and} \quad \forall q \in Q \tag{7}$$

$$\mathcal{L}_r^h(\mathbf{v}_h, q) \leq \mathcal{L}_r^h(\mathbf{v}_h, p_h) \leq \mathcal{L}_r^h(\mathbf{u}, p_h),$$

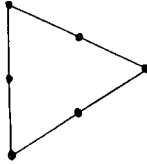
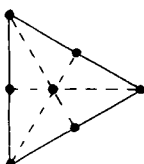
with

$$\mathcal{L}_r^h(\mathbf{v}_h, p_h) = \frac{\mu}{2}((\mathbf{v}_h, \mathbf{v}_h)) - (\mathbf{F}, \mathbf{v}_h) + (p_h, \operatorname{div}_h \mathbf{v}_h) + r(\operatorname{div}_h \mathbf{v}_h, \operatorname{div}_h \mathbf{v}_h).$$

And (7) is solved using the Uzawa algorithm, which leads to a statement of the numerical problem as follows, where the upper index (n) gives the step in the Uzawa algorithm: $\mathbf{v}_h^{(n)}$ and $p_h^{(n)}$ are presumed known; find $\mathbf{v}_h^{(n+1)} \in W$ so that

$$\forall \mathbf{u} \in W; \quad \frac{\mu}{2}((\mathbf{u}, \mathbf{v}_h^{(n+1)})) + r(\operatorname{div}_h \mathbf{u}, \operatorname{div}_h \mathbf{v}_h^{(n+1)}) = (\mathbf{u}, \mathbf{F}) - (\operatorname{div}_h \mathbf{u}, p_h^{(n)}) \tag{8a}$$

Table I

Kind of finite element	Space W defined by	Space Q defined by	div_h defined by
 <p>(without bubble function)</p>	<p>On each element, velocity components are defined by traditional quadratic interpolation on the six nodes: the three vertices and the three midpoints on each edge. The velocity is continuous from one element to the next</p>	<p>The pressure is constant on each element, but discontinuous from one element to the next</p>	<p>The average condition $\int \text{div } v_h \, d\Omega = 0$ (each element)</p>
 <p>(with bubble function)</p>	<p>The previous approximation plus a supplementary term of order three, the bubble function.^{3,5} The velocity is continuous from one element to the next.</p>	<p>The pressure is a linear function on each element (linear interpolation on the three vertices). The pressure is then discontinuous from one element to the next.</p>	<p>The average condition $\int q \, \text{div } v_h \, d\Omega = 0$ (each element) (for all linear functions q)</p>

and then find $p_h^{(n+1)} \in Q$ so that

$$\forall q \in Q; (q, p_h^{(n+1)} - p_h^{(n)}) = c(q, \text{div}_h v_h^{(n+1)}), \tag{8b}$$

c being a convergence parameter to be chosen.

And with matrix notations, the formulations (8a) and (8b) lead to the following two linear systems in $v_h^{(n+1)}$ and $p_h^{(n+1)}$, vectors of \mathbb{R}^m

$$\begin{aligned} \mathbf{u}^T \mathbf{A} v_h^{(n+1)} + r \mathbf{u}^T \mathbf{D}^T \mathbf{D} v_h^{(n+1)} &= \mathbf{u}^T \mathbf{F}_h - \mathbf{u}^T \mathbf{D}^T \mathbf{M} p_h^{(n)}, \\ \mathbf{q}^T \mathbf{M}^T \mathbf{M} (p_h^{(n+1)} - p_h^{(n)}) &= c \mathbf{q}^T \mathbf{M}^T \mathbf{D} v_h^{(n+1)} \end{aligned}$$

(\mathbf{u}^T denotes the transposed matrix of \mathbf{u}). By simplifying \mathbf{u}^T and \mathbf{q}^T we obtain

$$\begin{aligned} \mathbf{A}_r v_h^{(n+1)} &= \mathbf{F}_h - \mathbf{G}^T p_h^{(n)}, \\ \mathbf{B} (p_h^{(n+1)} - p_h^{(n)}) &= c \mathbf{G} v_h^{(n+1)}, \end{aligned}$$

with $\mathbf{A}_r = \mathbf{A} + r \mathbf{D}^T \mathbf{D}$, $\mathbf{G} = \mathbf{M}^T \mathbf{D}$ and $\mathbf{B} = \mathbf{M}^T \mathbf{M}$.

Note that \mathbf{A} is a symmetric, positive definite matrix. Thus \mathbf{A}_r is also symmetric. This traditional problem, with a symmetric positive definite matrix \mathbf{A} and \mathbf{M} reduced to the scalar 1, is studied in detail in Reference 2, where convergence of the Uzawa algorithm is studied (in spectral terms), giving the results as plotted in Table 2, in which $\lambda_m > 0$ is the smallest eigenvalue of \mathbf{A} and $\lambda_M > 0$ is the biggest eigenvalue of \mathbf{A} .

In conclusion, the case $r \neq 0$ seems to be more suitable than $r = 0$ for the Stokes problem, and more suitable as r increases. Nevertheless we should mention that the matrix \mathbf{A}_r becomes ill-conditioned for large values of r . So an upper limit exists on the choice of r .

Now it is interesting to look at our particular problem.

Table II

Parameter r	0	r
Optimum parameter c	$c_{\text{opt}} = \frac{2}{\lambda_m + \lambda_M}$	$c_{\text{opt}} = r + \frac{2 + r(\lambda_m + \lambda_M)}{2r\lambda_m\lambda_M + \lambda_m + \lambda_M}$
Rate of convergence with $c = c_{\text{opt}}$	$\leq \frac{1 - \lambda_m/\lambda_M}{1 + \lambda_m/\lambda_M}$	$\leq \frac{1 - \lambda_m/\lambda_M}{1 + \lambda_m/\lambda_M + 2r\lambda_m}$

Extension of these results to our problem

Our problem is different from the traditional homogeneous Stokes problem on three main points:

- (a) the Ω -periodicity boundary condition.
- (b) The unknown functions are complex.
- (c) The problem has a supplementary dynamic term. This quantity introduces a coupling effect between real and imaginary parts of the complex-valued unknown functions, so the problem becomes non-symmetric.

The results of the Lagrangian formulation (5) solved by the Uzawa algorithm and applied to our case were given in Reference 1. We shall now perform a similar extension and application using the augmented Lagrangian formulation (6) and the Uzawa algorithm.

The discrete problem to be solved can be written in a similar way to (8): $\mathbf{v}_h^{(n)}$ and $p_h^{(n)}$ are presumed known and complex-valued. Find $\mathbf{v}_h^{(n+1)}$ so that

$$\forall \mathbf{u} \in \mathbf{W}; \quad \frac{\mu}{2}((\mathbf{u}, \mathbf{v}_h^{(n+1)})) + i\omega\rho(\mathbf{u}, \mathbf{v}_h^{(n+1)}) + r(\text{div}_h \mathbf{u}, \text{div}_h \mathbf{v}_h^{(n+1)}) = (\mathbf{u}, \mathbf{F}) - (\text{div}_h \mathbf{u}, p_h^{(n)}) \quad (9)$$

and then find $p_h^{(n+1)}$ so that

$$\forall q \in \mathbf{Q}; (q, p_h^{(n+1)} - p_h^{(n)}) = c(q, \text{div}_h \mathbf{v}_h^{(n+1)}),$$

where $\mathbf{u}, \mathbf{v}^{(n+1)}, \mathbf{v}^{(n)}, q, p^{(n)}, p^{(n+1)}$ are complex-valued quantities which are chosen in suitable finite spaces with suitable scalar products.

As previously, by separating real and imaginary parts, using matrix block notations we can express the two linear systems, with real values to be solved, thus:

$$\begin{aligned} & \{\bar{\mathbf{u}}_1^T, \bar{\mathbf{u}}_2^T\} \begin{bmatrix} \mathbf{A} & \mathbf{0} \\ \mathbf{0} & \mathbf{A} \end{bmatrix} \begin{Bmatrix} \mathbf{v}_{h1}^{(n+1)} \\ \mathbf{v}_{h2}^{(n+1)} \end{Bmatrix} + \omega\rho\{\bar{\mathbf{u}}_1^T, \bar{\mathbf{u}}_2^T\} \begin{bmatrix} \mathbf{0} & -\mathbf{J} \\ \mathbf{J} & \mathbf{0} \end{bmatrix} \begin{Bmatrix} \mathbf{v}_{h1}^{(n+1)} \\ \mathbf{v}_{h2}^{(n+1)} \end{Bmatrix} \\ & + r\{\bar{\mathbf{u}}_1^T, \bar{\mathbf{u}}_2^T\} \begin{bmatrix} \mathbf{D}^T \mathbf{D} & \mathbf{0} \\ \mathbf{0} & \mathbf{D}^T \mathbf{D} \end{bmatrix} \begin{Bmatrix} \mathbf{v}_{h1}^{(n+1)} \\ \mathbf{v}_{h2}^{(n+1)} \end{Bmatrix} = \{\bar{\mathbf{u}}_1^T, \bar{\mathbf{u}}_2^T\} \begin{Bmatrix} \mathbf{F}_{h1} \\ \mathbf{Q} \end{Bmatrix} - \{\bar{\mathbf{u}}_1^T, \bar{\mathbf{u}}_2^T\} \begin{bmatrix} \mathbf{D}^T \mathbf{M} & \mathbf{0} \\ \mathbf{0} & \mathbf{D}^T \mathbf{M} \end{bmatrix} \begin{Bmatrix} \mathbf{p}_{h1}^{(n)} \\ \mathbf{p}_{h2}^{(n)} \end{Bmatrix} \end{aligned}$$

and

$$\{\bar{\mathbf{q}}_1^T, \bar{\mathbf{q}}_2^T\} \begin{bmatrix} \mathbf{M}^T \mathbf{M} & \mathbf{0} \\ \mathbf{0} & \mathbf{M}^T \mathbf{M} \end{bmatrix} \begin{Bmatrix} \mathbf{p}_{h1}^{(n+1)} - \mathbf{p}_{h1}^{(n)} \\ \mathbf{p}_{h2}^{(n+1)} - \mathbf{p}_{h2}^{(n)} \end{Bmatrix} = c\{\bar{\mathbf{q}}_1^T, \bar{\mathbf{q}}_2^T\} \begin{bmatrix} \mathbf{M}^T \mathbf{D} & \mathbf{0} \\ \mathbf{0} & \mathbf{M}^T \mathbf{D} \end{bmatrix} \begin{Bmatrix} \mathbf{v}_{h1}^{(n+1)} \\ \mathbf{v}_{h2}^{(n+1)} \end{Bmatrix},$$

where the suffix 1 denotes the real part, the suffix 2 denotes the imaginary part, and $\bar{\mathbf{u}}_1$ is the vector whose components are the conjugate complex numbers of the corresponding components of the vector \mathbf{u}_1 .

By simplifying $\{\bar{\mathbf{u}}_1^T, \bar{\mathbf{u}}_2^T\}$ and $\{\bar{\mathbf{q}}_1^T, \bar{\mathbf{u}}_2^T\}$ we obtain as previously

$$\begin{bmatrix} \mathbf{A} + r\mathbf{D}^T\mathbf{D} & -\omega\rho\mathbf{J} \\ \omega\rho\mathbf{J} & \mathbf{A} + r\mathbf{D}^T\mathbf{D} \end{bmatrix} \begin{Bmatrix} \mathbf{v}_{h1}^{(n+1)} \\ \mathbf{v}_{h2}^{(n+1)} \end{Bmatrix} = \begin{Bmatrix} \mathbf{F}_{h1} \\ \mathbf{0} \end{Bmatrix} \begin{bmatrix} \mathbf{G}^T & \mathbf{0} \\ \mathbf{0} & \mathbf{G}^T \end{bmatrix} \begin{Bmatrix} \mathbf{p}_{h1}^{(n)} \\ \mathbf{p}_{h2}^{(n)} \end{Bmatrix},$$

$$\begin{bmatrix} \mathbf{B} & \mathbf{0} \\ \mathbf{0} & \mathbf{B} \end{bmatrix} \begin{Bmatrix} \mathbf{p}_{h1}^{(n+1)} - \mathbf{p}_{h1}^{(n)} \\ \mathbf{p}_{h2}^{(n+1)} - \mathbf{p}_{h2}^{(n)} \end{Bmatrix} = \begin{bmatrix} \mathbf{G} & \mathbf{0} \\ \mathbf{0} & \mathbf{G} \end{bmatrix} \begin{Bmatrix} \mathbf{v}_{h1}^{(n+1)} \\ \mathbf{v}_{h2}^{(n+1)} \end{Bmatrix}, \quad (10)$$

with $\mathbf{G} = \mathbf{M}^T\mathbf{D}$ and $\mathbf{B} = \mathbf{M}^T\mathbf{M}$.

The augmented Lagrangian formulation introduces the $r\mathbf{D}^T\mathbf{D}$ term on the diagonal blocks of the first linear system.

In the static case ($\omega = 0$) the Uzawa algorithm shows the same behaviour as for the homogeneous Stokes problem.

In the dynamic case ($\omega \neq 0$) the problem becomes non-symmetric and the results of the preceding subsection on the convergence of the Uzawa algorithm are no longer valid. Nevertheless the structure of the first linear system in (10) shows that augmented Lagrangian formulation is well-adapted to our problem. It is a well-known, simple and traditional technique which has here a particular interest for the following reason. In choosing values of the parameter r in such a way that the matrix

$$\begin{bmatrix} \mathbf{A} + r\mathbf{D}^T\mathbf{D} & -\omega\rho\mathbf{J} \\ \omega\rho\mathbf{J} & \mathbf{A} + r\mathbf{D}^T\mathbf{D} \end{bmatrix}$$

becomes pseudosymmetric (diagonal blocks $\mathbf{A} + r\mathbf{D}^T\mathbf{D}$ dissimulating other blocks $\omega\rho\mathbf{J}$) we can hope to increase the rate of convergence of the Uzawa algorithm. The structure of the dynamic problem (10) is then similar to the static one. We can hope to use the convergence results of the traditional homogeneous Stokes problem.

But for the non-symmetric case, by means of a spectral study of the convergence of the Uzawa algorithm, it is not possible to test our prediction. Experimentation and testing would therefore confirm our hope.

TEST ON A SIMPLE GEOMETRICAL CASE

In porous media, the flow is a significant result. The average velocity over a period $V_i^{(n)}$ gives the flow as follows, due to the spatial periodicity properties:

$$V_i^{(n)} = \frac{1}{|\Omega|} \int_{\Omega_i} v_{hi}^{(n)} d\Omega \quad (\text{for the } i\text{th component}),$$

(this is a complex number) where n is the number of steps in the Uzawa algorithm. The convergence of the Uzawa algorithm will then be tested with the parameter

$$\text{em } 1^{(n)} = \frac{1}{4} \sqrt{\left[\sum_{i=1}^2 (|V_i^{(n)}|^2 - |V_i^{(n-1)}|^2) \right]}$$

where $||$ represents the complex modulus. Numerical results will be compared to analytical ones, given by Avallet,⁸ in the case of a narrow slit (Figure 2).

The convergence of the Uzawa algorithm is proved, for our discrete problem when $0 < c < 4r + 2$. The proof can be extended from the static case,² as was done in Reference 1 for

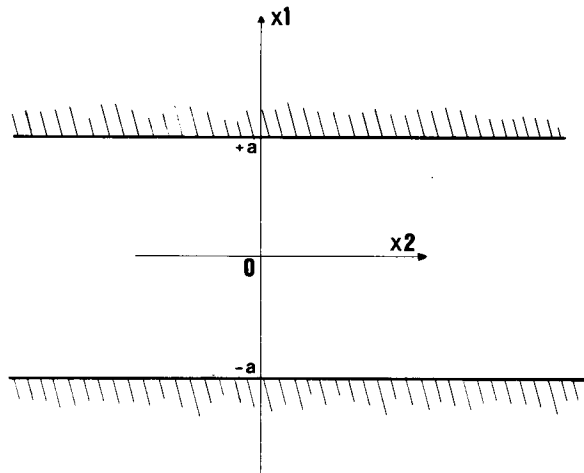


Figure 2. A narrow slit

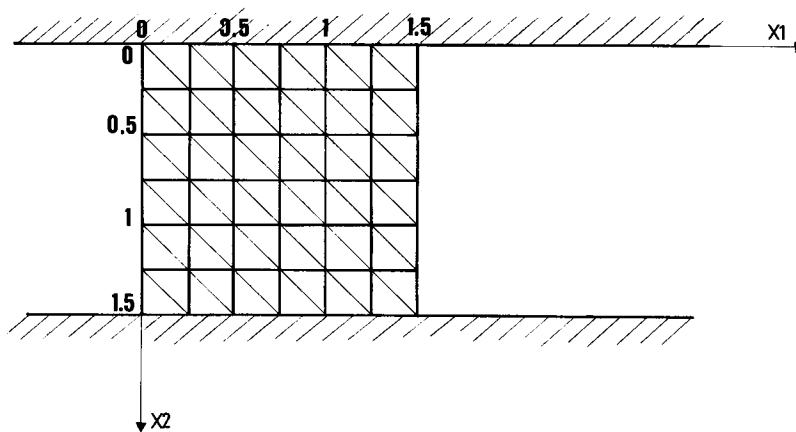


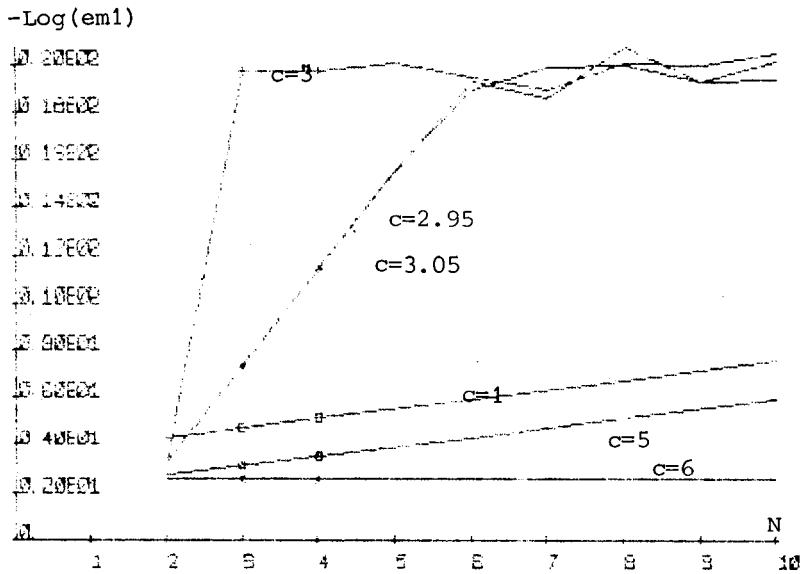
Figure 3. Mesh A for the narrow slit

the traditional Lagrangian formulation. Note that discretization using bubble functions modifies the proof. Nevertheless, the results are still valid. Obviously, in the case of computations without bubble functions, and with $\omega = 0$, we must check all traditional theoretical results in Reference 2.

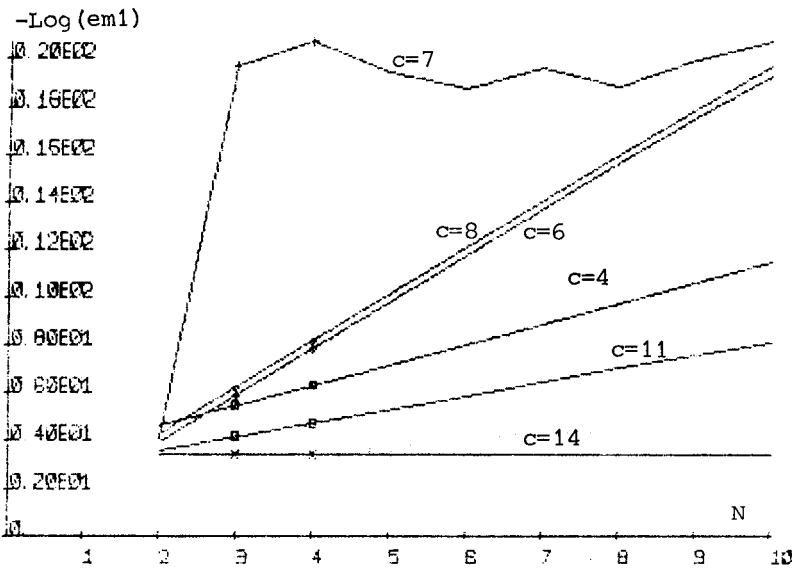
The static case, $\omega = 0$

In this case, we do not need computations with a bubble function to approximate the analytical solutions which are quadratic in velocity and constant in pressure. Many computations were performed for various parameters r and c , without bubble functions and with mesh A, as in Figure 3. Figures 4 and 5 give the convergence of the Uzawa algorithm by plotting the parameter ϵm_1 against the iteration number N for various values of r and c .

The simplicity of the analytical solutions means that, the numerical results agree closely with



(a)



(b)

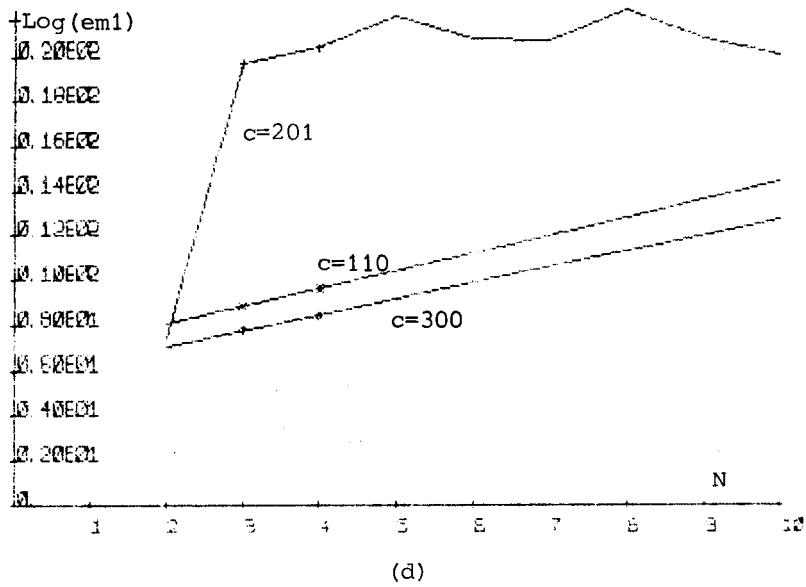
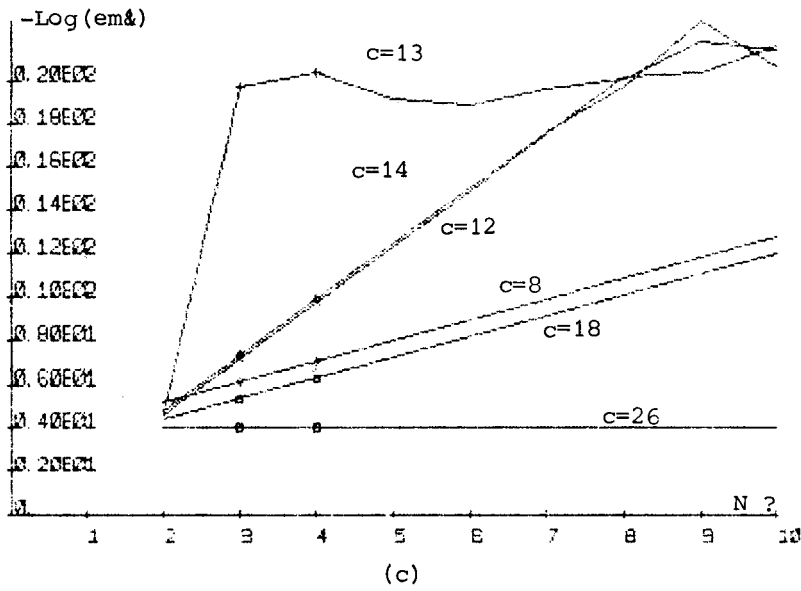


Figure 4. $-\log(\text{em})$ against the number of iterations N with $\omega=0$, for several values of c and for computations without bubble functions (a) with $r=1$; (b) with $r=3$; (c) with $r=6$; (d) with $r=100$

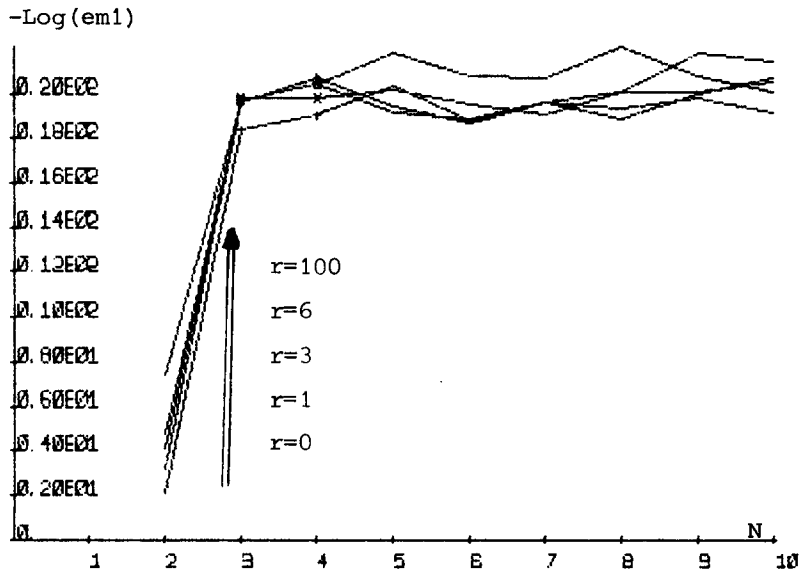


Figure 5. $-\log(\text{em}1)$ against the number of iterations N with $\omega = 0$, for $c = c_{\text{opt}}$ various values of r and for computations without bubble functions

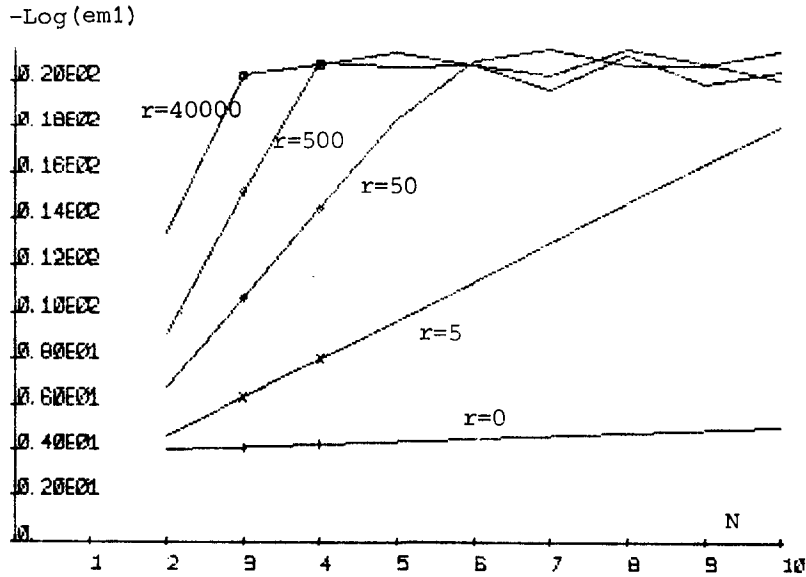
Table II			Table III			
r	0	1	r	3	6	100
Numerical value of c_{opt}	1	3	Numerical value of c_{opt}	7	13	201
$\lambda_m \approx 0$ ($0 < \lambda_m < 1$) $\lambda_M \approx 2$			Theoretical value: $c_{\text{opt}} = r + \frac{2 + r(\lambda_m + \lambda_M)}{2r\lambda_m\lambda_M + (\lambda_m + \lambda_M)}$	7	13	201

theoretical predictions. Moreover the convergence of the Uzawa algorithm is fast and the influence of r is low. The preconditioning technique is useless in this case, because the problem remains well-conditioned. Nevertheless, in this case, we tested our computations with the spectral study² of the Uzawa algorithm convergence given in Table II. The optimum parameter $c = c_{\text{opt}}$, for a given value of r , is determined by experimentation. Results for $r = 0$ and $r = 1$ are used to compute values of λ_m and λ_M . Theoretical predictions of c_{opt} for other values of r are then deduced and compared to experimental data. These results are given in Table III.

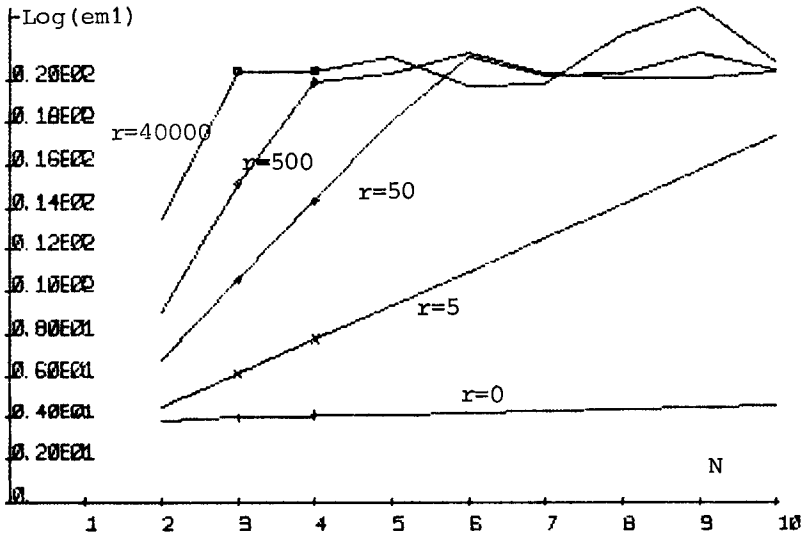
The dynamical case, $\omega \neq 0$

The (non-symmetric) structure of the matrix A_r of the linear system (10) does not permit a theoretical study of the Uzawa algorithm's convergence. However, experimental investigations are

useful. Figures 6–8 give these results in the same way as Figures 4 and 5 applied to the static case ($\omega = 0$).

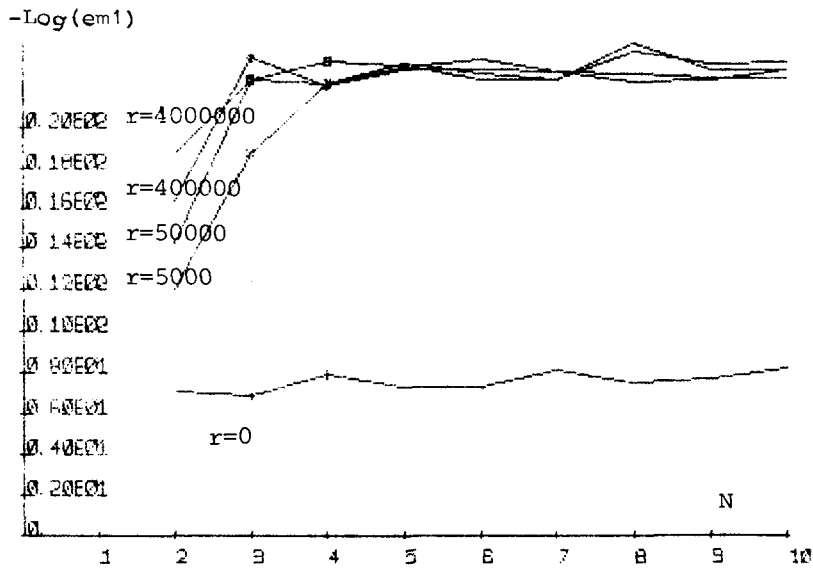


(a)

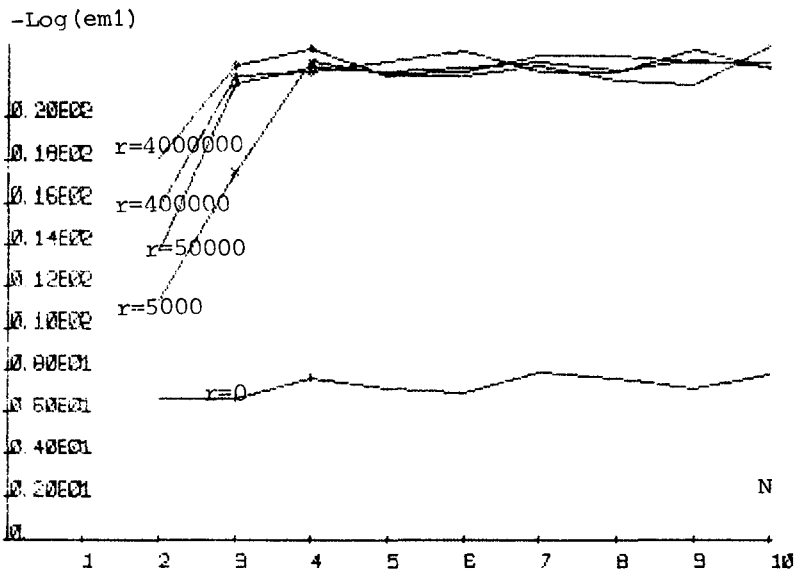


(b)

Figure 6. $-\log(em1)$ against the number of iterations N with $\omega = 5$, for $c = c_{opt}$ and for various values of r : (a) computations without bubble functions; (b) computations with bubble functions



(a)



(b)

Figure 7. $-\log(em1)$ against the number of iterations N with $\omega = 50$, for $c = c_{opt}$ and for various values of r ; (a) computations without bubble functions; (b) computations with bubble functions

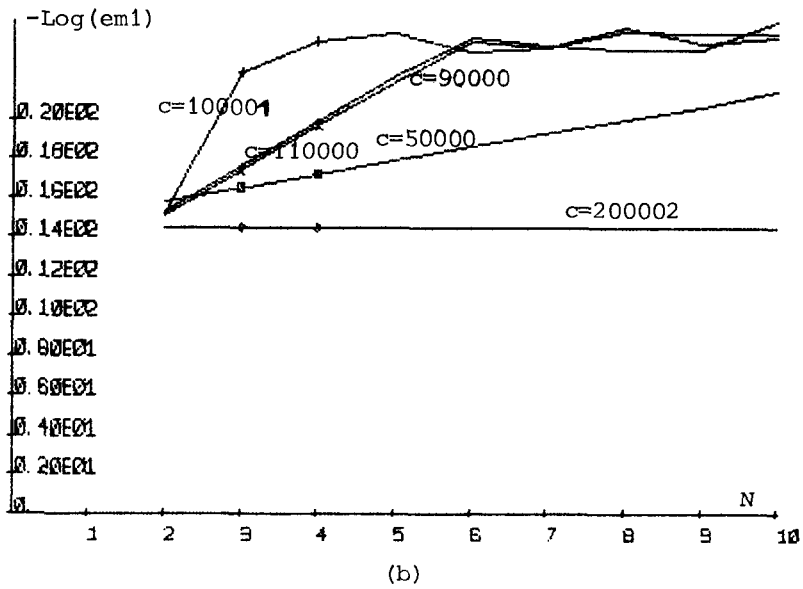
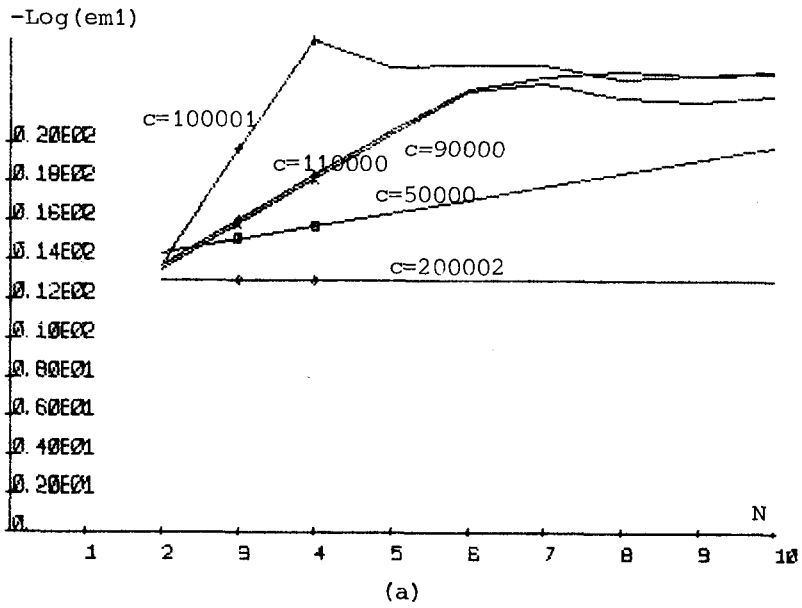


Figure 8. $-\log (em_1)$ against the number of iterations N with $\omega = 500$, $r = 50,000$ and for various values of c ; (a) computations with bubble functions; (b) computations without bubble functions

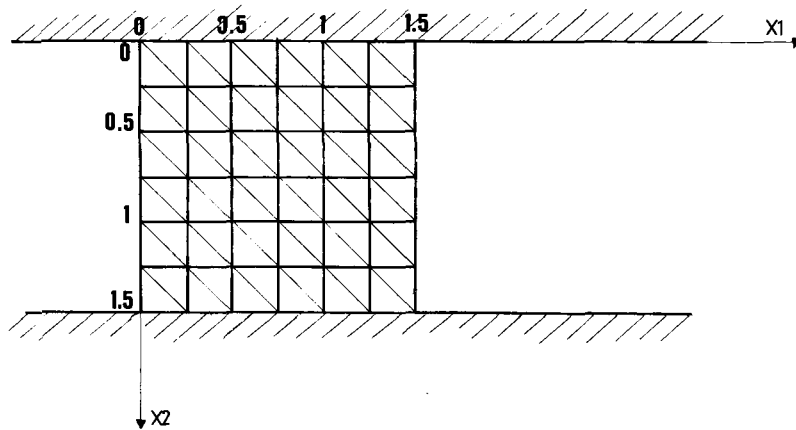


Figure 9. Mesh B for the narrow slit

These numerical experiments confirm our hopes. The behaviour of the Uzawa algorithm for the static case ($\omega = 0$, real unknowns) can be extended to the dynamic case ($\omega \neq 0$, complex unknowns) provided that we choose a suitable parameter r . The simple rule $r = 100\omega$ gives good results. In this case the optimum parameter c_{opt} is predicted as for the static case ($c_{opt} = 2r + 1$ for our discrete problem). Nevertheless, as for the usual static case, we must be wary of the accuracy of the results for large values of r . This is illustrated by an example given in Table IV. Table V shows that, with increased frequencies, the mesh should be refined to obtain accurate numerical solutions.

NUMERICAL EXPERIMENT

In this last part, we present computations for a severe geometrical case (Figure 10), in order to improve the numerical scheme employed. Figures 11 and 12 give these results in dimensionless form as previously.¹ At low frequencies, numerical values are confirmed and, as in Reference 1, agree closely with experimental data. At high frequencies, no significant experimental data are available at the present time. Nevertheless a theoretical model is possible.^{9,10} Computations with the augmented Lagrangian formulation are also possible and correspond closely to such analytical predictions.

Moreover faithful numerical results are reached after about only five steps in the Uzawa algorithm. For various pulsations ω , Table VI gives the number of iterations N needed to obtain a solution for various pairs (r, c) .

On the other hand, there still remains a problem, i.e. the size of the discrete problem (memory storage). Consequently, suitable refinements in the mesh are not always possible. For instance, a mesh as in Figure 10 leads to 5580 degrees of freedom.

CONCLUSION

The use of complex unknown functions, coupled with this simple technique, seems to be an efficient method of solving this periodic, harmonic Navier–Stokes problem. The interest of the augmented Lagrangian technique is obvious. With a suitable parameter r , numerical behaviour of the Uzawa algorithm in the dynamic case is similar to that in the static case.

Of course, as mentioned by Fortin and Glowinski² for the usual homogeneous Stokes problem,

Table IV. Velocity components after ten steps of the Uzawa algorithm for $\omega = 50$. All computations are with $c = c_{opt}$. So convergence of the Uzawa algorithm is reached after ten iterations

Computation type	r	$c = c_{opt}$ ($= 2r + 1$)	Real part of $V_1^{(10)}$	Real part of $V_2^{(10)}$	Imaginary part of $V_1^{(10)}$	Imaginary part of $V_2^{(10)}$
Mesh A without bubble functions	5000	10,001	-0.1496×10^{-2}	0.2247×10^{-5}	0.1791×10^{-1}	-0.1941×10^{-4}
Mesh A without bubble functions	50,000	10,001	0.1498×10^{-2}	0.2035×10^{-5}	0.1791×10^{-1}	-0.1935×10^{-4}
Mesh A without bubble functions	4×10^5	8×10^5	-0.1474×10^{-2}	0.4015×10^{-5}	0.1792×10^{-1}	-0.1870×10^{-4}
Mesh A without bubble functions	4×10^6	8×10^6	-0.1426×10^{-2}	0.1080×10^{-4}	0.1793×10^{-1}	-0.1433×10^{-4}
Theoretical results			-0.1886×10^{-2}	0	0.1811×10^{-1}	0
Mesh A with bubble functions	4×10^6	8×10^6	-0.1021×10^{-2}	-0.7021×10^{-11}	0.1794×10^{-1}	0.3741×10^{-10}
Mesh A with bubble functions	4×10^5	8×10^5	-0.1590×10^{-2}	-0.8394×10^{-11}	0.1794×10^{-1}	-0.3557×10^{-11}
Mesh A with bubble functions	50,000	100,001	-0.1564×10^{-2}	-0.6759×10^{-11}	0.1795×10^{-1}	0.1288×10^{-10}
Mesh A with bubble functions	5000	10,001	-0.1568×10^{-2}	-0.1490×10^{-10}	0.1795×10^{-1}	0.8292×10^{-10}
Mesh B with bubble functions	5000	10,001	-0.1834×10^{-2}	0.2302×10^{-11}	0.1812×10^{-1}	-0.3212×10^{-10}

Table V. Velocity components after 10 steps of the Uzawa algorithm for $\omega = 500$

Computation type	r	$c = c_{\text{opt}} (= 2r + 1)$	Real part of		Imaginary part of	
			$V_1^{(10)}$	$V_2^{(10)}$	$V_1^{(10)}$	$V_2^{(10)}$
Theoretical results			-5.9631×10^{-5}	0	1.9404×10^{-3}	0
Mesh A without bubble functions	50,000	100,001	-2.0250×10^{-5}	-0.50×10^{-6}	1.8437×10^{-3}	-0.15×10^{-4}
Mesh A with bubble functions	50,000	100,001	-2.4084×10^{-5}	-0.28×10^{-11}	1.8593×10^{-3}	-0.50×10^{-12}
Mesh B with bubble functions	50,000	100,001	-3.8086×10^{-5}	-0.83×10^{-12}	1.9184×10^{-3}	0.49×10^{-11}

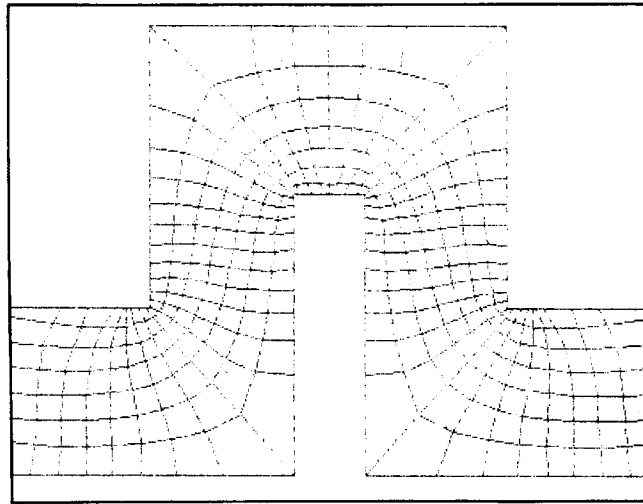


Figure 10. The period Ω to be studied and the associated mesh

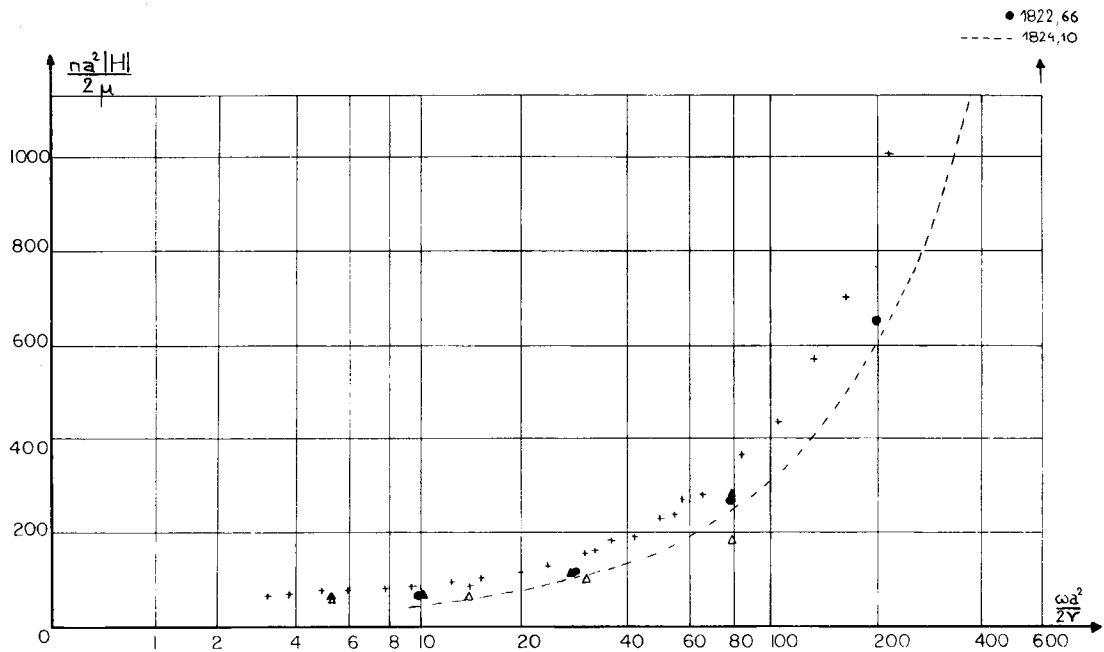


Figure 11. The complex modulus of the dimensionless ratio of body force $F|_0 F_1$ to the average velocity $V|_0 V_1$ against dimensionless pulsation: + experimental data (wrong at high frequencies); Δ previous results with $r=0$ without bubble functions; \blacktriangle previous results with $r=0$ with bubble functions; \bullet new results with $r=10,000$ with bubble functions; -----theoretical modelling for large pulsations¹

other algorithms are available to solve the augmented Lagrangian formulation and give a faster convergence. But these refinements require an increase in memory size. For instance, if we consider the comparative study of chapter 2 of Reference 2, the conjugate gradient method allows the best

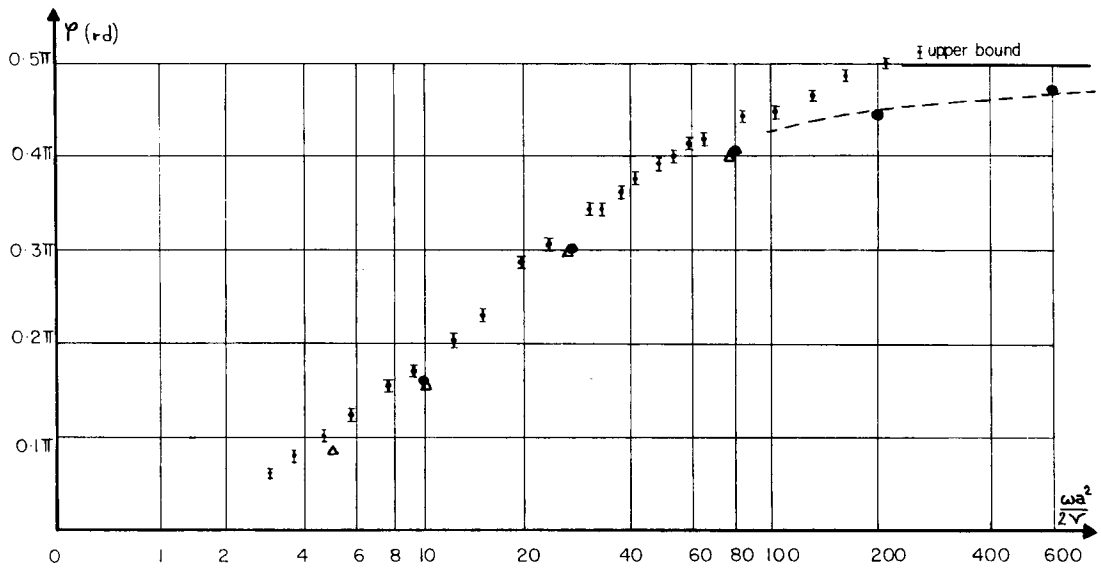


Figure 12. Phase of the ratio (F_1/V_1) against dimensionless pulsations: \times experimental data (wrong at high frequencies); Δ previous results with $r=0$, with bubble functions; \bullet new results with $r=10,000$, with bubble functions; ----theoretical modelling for high pulsations

Table VI

ω	r	c	Iteration number N
0	0	1	50
0	1000	2001	5
0	10,000	20,001	5
10	0	1.5	140
10	10,000	20,001	5
27	0	1.8	200
27	10,000	20,001	5
78	10,000	20,001	5
200	10,000	20,001	5
600	10,000	20,001	5

(These computations with a bubble function and the mesh of Figure 10 are always performed with the same initial pressure distribution.)

rate of convergence for the traditional Stokes problem. At each step of the algorithm we need to store in memory two additional vectors, whose dimensions are those of the discrete velocity vector. The rate of convergence is then roughly doubled compared to the traditional Uzawa algorithm we used. In our case, the size of the discrete problem is a sizeable restriction.

The conforming finite elements of Crouzeix and Raviart, extended to complex unknown functions, rapidly provide a large linear system. Moreover experiments at high frequencies show that refinements in the mesh are required to obtain a good approximation, but are not always possible because of the size of the discrete problem. Nevertheless, use of bubble functions provides a partial answer to this problem at lower cost. What is most needed here is memory capacity. Further investigations would surely be better aimed at trying to reduce the size of the problem by using other finite elements (e.g. non-conforming finite elements).

Finally we would like to comment on how to obtain an accurate numerical solution with our scheme:

- (a) Computations with bubble functions should be used.
- (b) With increased frequencies, the mesh should be refined.
- (c) $r = 100\omega$ should be chosen.
- (d) It is advisable to choose $c = c_{\text{opt}} = 2r + 1$ for our dimensionless problem.

REFERENCES

1. L. Borne, R. Chambon and J. L. Auriault, 'Conforming finite element computations applied to a spatially periodic, harmonic Navier–Stokes problem', *Int. j. numer. methods in fluids*, **5**, 685–707 (1985).
2. M. Fortin and R. Glowinski, 'Méthodes de Lagrangien augmenté. Applications a la résolution numérique de problèmes aux limites', Dunod-collection *Méthodes Mathématiques de l'informatique* sous la direction de J.-L. Lions, 1982.
3. R. Temam, *Navier–Stokes Equations*, North Holland, Amsterdam, 1977.
4. H. Uzawa, L. Hurwicz and J. K. Arrow, *Studies in Linear and Non-Linear Programming*, Stanford University Press, Stanford, California, 1958.
5. M. Crouzeix and P. A. Raviart, 'Conforming and non-conforming finite element methods for solving the stationary STOKES equations', *R.A.I.R.O., Analyse Numerique*, **3**, 33–76 (1973).
6. I. Babuska, 'Error bounds for finite element method', *Numer. Math.*, **16**, 322–333 (1971).
7. F. Brezzi, 'On the existence, uniqueness and approximation of saddle-point problems, arising from Lagrangian multipliers', *Revue Francaise d'automatisme Informatique Recherche Opérationnelle, Analyse Numerique*, **8**, (R-Z) 129–151 (1974).
8. C. Avallet, 'Comportement dynamique de milieux poreux saturés déformables', *Thèse 3ème cycle*, Grenoble, 1981.
9. J. L. Auriault, L. Borne and R. Chambon, 'Dynamics of porous saturated media, checking of the generalized law of Darcy', *J. Acoust. Soc. Am* **77** (5), 1641–1650 (1985).
10. L. Borne, 'Contribution à l'étude du comportement dynamique des milieux poreux saturés déformables', *Thèse Doc. Ingenieur*, Grenoble, 1983.